Journal of Sound and Vibration (2002) **250**(4), 745–761
doi:10.1006/jsvi.2001.3602, available online at http://www.idealibrary.com on IDEAL®

LETTERS TO THE EDITOR

LOSS FACTORS OF COMPOSITE HONEYCOMB SANDWICH PANELS

K. Renji and S. Shankar Narayan

Structures Group, ISRO Satellite Centre, Bangalore, India, 560017. *E-mail*: *renji@isac.ernet.in*

(*Received* 2 *January* 2001)

1. INTRODUCTION

Statistical Energy Analysis (SEA), developed by Lyon [1] and others, is widely used in evaluating the response of complex structures subjected to high-frequency excitations. In SEA, the entire system is considered to be an assembly of a number of structural elements, called subsystems. Power balance of these subsystems forms the basis for the SEA calculations. Modal density, dissipation loss factor and coupling loss factor of the subsystems/subsystem connectivity form the important SEA parameters. Accuracy of the prediction of response using SEA greatly depends on, other than the limitations of SEA, the accuracy with which these SEA parameters are estimated. For reliable prediction of structural fatigue life, Lyon [1] suggests that the response has to be estimated within an accuracy of 1 dB which needs that the SEA parameters also be estimated within such an accuracy.

The dissipation loss factor is a measure of the power dissipated within a subsystem. Bakel and Vries [2] discussed the sensitivity of the SEA results to the dissipation loss factor. Response of a subsystem is greatly influenced by the dissipation loss factor. In most of the situations the dissipation loss factor can be obtained only by conducting experiments on either the given structure or identical/similar structures.

Many of the spacecraft structural components are made of honeycomb sandwich panels. Some of the examples of honeycomb sandwich construction include the equipment panels, payload platforms, solar panels and antenna reflectors. In particular, solar panels, antenna reflectors, etc., have face sheets made of composite material for optimum performance. These elements have large area and low mass and hence their dynamic response levels can be significant when they are subjected to acoustic excitation. Hence, for such elements the estimation of the response to acoustic excitation is very important. To use SEA for the above purpose, it is essential to determine the dissipation loss factors of composite honeycomb sandwich panels.

Cummins and Farrow [3] and Eaton [4] presented a compilation of the dissipation loss factors of some of the spacecraft structural elements. For honeycomb sandwich panels, they suggest a value of 0·020 for the dissipation loss factor. Ranky and Clarkson [5] obtained a similar value of dissipation loss factor for honeycomb sandwich panels. All the above experiments were conducted in air and hence the reported loss factors were the total loss factors, that is the sum of the dissipation loss factor and the radiation loss factor. Clarkson and Brown [6] have shown that the use of the total loss factor as the dissipation loss factor can lead to large errors in the estimated response. The radiation loss factor can be significant, especially for the honeycomb sandwich panels. Clarkson and Brown [6]

0022-460X/02/090745 + 17 $35.00/0

reported a value of 0·002 as the dissipation loss factor of honeycomb sandwich panels after removing the radiation loss factor component. One can observe that this value of the dissipation loss factor is very small compared to those reported by Cummins and Farrow [3].

One important type of construction of interest is the honeycomb sandwich panel with composite face sheets. The references [3, 4] suggest the use of 0·020 as the loss factor of such panels and a value of 0·030 for solar panels. But these are obtained from tests using propagating wave tube and hence not suitable for using in SEA-based calculations though they can be used for acoustic absorption studies. There is no information available on the dissipation loss factor of such panels obtained using energy method or transient decay method, which are generally used for this purpose. Hence, there is a need to determine the dissipation loss factors of such panels. The present paper is a contribution in this regard.

To determine the loss factor using the energy method, excitation force has to be measured. The excitation force is usually measured using impedance head. But the mass of the impedance head and the attachment elements like the stud and cube can influence the measured force. Hence, to obtain the actual force, correction factors need to be applied on the measured force. These correction factors are derived in this paper. The results show that if these corrections are not applied, the measured loss factors of honeycomb sandwich panels are in large error.

Hence, the present paper presents the dissipation loss factors of honeycomb sandwich panels with composite face sheets. Expression for the correction to be applied on the measured force in order to determine the actual force is developed in this study. Use of this expression shows the importance of the correction to be applied when using impedance head for measuring force.

2. EXPERIMENTAL TECHNIQUE

The dissipation loss factor is a measure of the energy dissipated within a subsystem. By definition, the dissipation loss factor is the ratio of the power dissipated within the subsystem per unit frequency in rad/s, to the mean energy of the subsystem. The dissipation loss factor of subsystem denoted by η_d is then given by

$$\eta_d = \pi_d/(\omega E), \tag{1}$$

where π_d is the mean power dissipated within the subsystem and E is the mean energy of the subsystem at a frequency ω rad/s. In other words, the power dissipated within a subsystem is equal to $\omega\eta_d E$. In SEA, twice the mean kinetic energy is taken as the mean energy of the subsystem [7]. The mean energy of the subsystem having a mass of m and spatial average of the mean square value of the velocity $\langle v^2 \rangle_x$ can then be shown to be [1]

$$E = m\langle v^2 \rangle_x. \tag{2}$$

The dissipation loss factor can be obtained experimentally either using steady state techniques or using transient techniques. The steady state techniques include the half-power bandwidth method and the energy method.

In the case of the half-power bandwidth method, the loss factor is calculated from the measured frequency response function using the relation

$$\eta_d = \Delta/f_n, \tag{3}$$

where Δ is the half-power bandwidth and f_n is the natural frequency. The half-power bandwidth technique is suitable only when the modes are well separated, in other words if the modal overlap is less than unity. This technique gives only the modal loss factor and this can be determined using either sine sweep or random excitation.

While using the energy method, the response levels at several locations are measured for a known input power. From the equality of the input power and the dissipated power, the dissipation loss factor is obtained. In other words for an input power of π_{in}, the dissipation loss factor is given by

$$\eta_d = \pi_{in}/(\omega m \langle v^2 \rangle_x). \tag{4}$$

If the structure is excited by a shaker, by measuring the input power and the spatial average of the mean square value of the velocity response of the structure, the dissipation loss factor of the structure can be determined using equation (4). The loss factor can be obtained by using either sine sweep excitation or random excitation. The energy method can give the loss factor at each frequency and hence at low frequencies the method can be used to get the modal loss factor.

The energy method can be used even in the frequency range where the modal overlap is large. At higher frequencies the mean input power can be determined using the relation [1, 8]

$$\pi_{in} = f_p^2 n(f)/(4m), \tag{5}$$

where f_p^2 is the mean square value of the excitation force and $n(f)$ is the modal density of the structure at a frequency f. Substituting the expression for the power input in equation (4), the expression for the loss factor becomes

$$\eta_d = f_p^2 n(f)/\{8\pi f m^2 \langle v^2 \rangle_x\}. \tag{6}$$

Clarkson and Pope [9] demonstrated this technique for plates and cylinders. This method assumes that the modal responses are independent and there is no inter-modal coupling [10].

In the case of transient technique the loss factor is determined from the decay of the response level when the excitation is suddenly stopped. This technique is also known as envelope decay method. The loss factor is then obtained from the reverberation time or the decay rate. Reverberation time, denoted by T_{60}, is the time required for the response level to be dropped by 60 dB and the decay rate, denoted by DR, is the drop in the response level expressed in terms of dB in unit time. The dissipation loss factor is related to these parameters by

$$T_{60} = 2{\cdot}2/(f\eta_d), \tag{7}$$

$$DR = 27{\cdot}3 f\eta_d. \tag{8}$$

Usually, decay rate is specified for structural systems and reverberation time is specified for acoustic fields. One can obtain the modal loss factor by exciting the required mode using sine excitation. The average value of the modal loss factors gives the frequency averaged loss factor. This procedure is particularly suitable for the lower order modes. On the other hand, random excitation in the frequency band of interest can be applied and the frequency-averaged loss factors can be obtained from the decay of the mean square values of the response levels. The decay data can become corrupted by the modes of vibration which are excited due to the transients generated by the cutting-off of the excitation. The dissipation loss factor obtained using the decay method is dominated by the lower values of the loss factors.

While using the contact-type excitation, the damping due to the contact could be significant and corrupt the measured loss factor especially in the case of a structure with very low value of damping. As Bies and Hamid [11] suggested, use of shakers with non-contacting electromagnet is advisable in such situations. But this can introduce eddy current damping. Contact-type excitation is used in the present study.

In SEA-based calculations, we require frequency-averaged loss factors. In the frequency range, where there is large modal overlap the frequency-averaged loss factor is only meaningful. In the energy method this can be achieved using the frequency averaging or using random excitation with suitable bandwidths. While using the half-power bandwidth method, the frequency-averaged loss factor can be obtained from the modal loss factor by taking the energy average. Ranky and Clarkson [5] pointed out that in SEA based calculations, energy average is the most appropriate averaging. This can be directly obtained when the energy method is used. Ranky and Clarkson [5] demonstrated that there was no significant difference between the results obtained using the energy method and the decay method if the modes in the bands had similar values of loss factors. If the modes in the bands do not have similar values of loss factors, the energy method gives the required result for use in SEA. Hence, the energy method is preferred. In the present experiments energy method is used to determine the loss factor.

There are some precautions to be taken while using the energy method in evaluating the loss factor. As Brown and Norton [12] suggested, since the driving point impedance is very small near the resonance and hence its measurement could be in error, driving point impedance should not be used in evaluating the input power. Since the measured velocity at the driving point include additional near field component, the velocity of the driving point should not be included in estimating the spatial averaged velocity as pointed out by Ranky and Clarkson [5]. Many of the experiments to obtain the dissipation loss factors are often conducted in air. In such situations, the input power is balanced by the dissipated power as well as the sound power radiated. Hence, the measured loss factor is the sum of the dissipation loss factor and the radiation loss factor. Clarkson and Brown [6] have shown that the use of the total loss factor as the dissipation loss factor can lead to large errors in the estimated response. To obtain the dissipation loss factor, one has to necessarily subtract the radiation loss factor from the total measured loss factor. The radiation loss factor can be theoretically estimated for simple structural forms. The radiation loss factor is significant near and above the critical frequency of the structure. For a thin plate the critical frequency is very high and hence the radiation loss factor is generally lower. But the critical frequencies of honeycomb sandwich panels are lower and hence the radiation loss factors can be significant. Hence, while obtaining the dissipation loss factors of honeycomb sandwich panels, care should be taken in removing the radiation loss factor component. All these precautions are taken in the present experiment.

3. DETAILS OF THE PANEL

The dissipation loss factor of a typical composite honeycomb sandwich panel is obtained experimentally using the technique discussed above. The structural details of the panel considered are given here. The panel considered is a solar panel of a typical spacecraft.

Dimensions	$2{\cdot}15 \times 1{\cdot}80$ m
Area	$3{\cdot}87$ m^2
Core material	Aluminium
Thickness of the core	18 mm
Core	3/8 − 5056 − 0·0007

Foil thickness of the core	0·018 mm
Cell size	9·54 mm
Density of the core	16 kg/m^3
Shear modulus of the core	$6{\cdot}32 \times 10^7$, $10{\cdot}53 \times 10^7$ N/m^2
Face sheet material	Two layers of (0/90) CFRP (Carbon Fibre Reinforced Plastics)
Thickness of the face sheet	0·2 mm
Mass of the panel	13·81 kg

At a few locations, local reinforcements are provided.

Each CFRP layer has the following properties:

Young's modulus along fibre direction	30×10^{10} N/m^2
Young's modulus along transverse direction	$0{\cdot}607 \times 10^{10}$ N/m^2
The Major Poisson ratio	0·346
Shear modulus	$0{\cdot}50 \times 10^{10}$ N/m^2

Calculated values of flexural and shear rigidity are:

D_{11}	5135 N m
D_{22}	5028 N m
D_{12}	69·74 N m
D_{66}	165·6 N m
N	15×10^5 N/m

For calculating the modal density, the mass of the panel is taken as 10·92 kg. This is obtained by neglecting the lumped masses, as suggested by Clarkson and Ranky [13], such as hinge inserts, hold-down inserts and doublers provided at a few locations.

4. EXPERIMENTAL RESULTS

The dissipation loss factor of the composite honeycomb sandwich panel whose details are given in section 3 is determined experimentally. The energy method discussed in section 2, that is equation (6), is employed in determining the loss factor. The panel is excited at a particular location using the shaker system and the excitation force is measured. From the measured acceleration response levels, the mean square value of the velocity response levels are calculated. As discussed earlier, the velocity at the driving point is not considered in determining the spatial average of the velocity. The experiment is repeated by exciting at a few other points and measuring the corresponding acceleration levels. The measured value of the force and the spatial average of the mean square value of the velocity response for different driving point locations are used in determining the loss factor. The information on the modal density, which is required to obtain the loss factor using equation (6), is theoretically estimated [14]. The tests are conducted in air.

4.1. TEST SET-UP

The panel is mounted on a fixture at six locations called hold-down points. The fixture in turn is mounted on a seismic mass. Figure 1 shows the test set-up. The panel is excited at four locations shown in Figure 2. An aluminium block is bonded on the panel and the panel is excited using electro-dynamic shaker connected to the block through a stringer. When the panel is excited at one location, the acceleration responses are measured at the other three locations which are used for determining the spatial-averaged velocity. The vibration response at the driving point is not used in determining the spatial-averaged velocity as

Figure 1. A view of the test set-up.

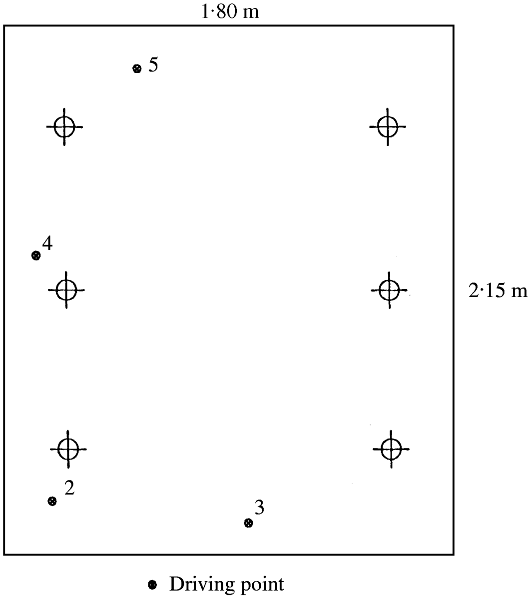

Figure 2. Driving point locations on the panel.

pointed out by Ranky and Clarkson [5]. Hence, in the present experiment the spatial-averaged velocity is determined from the acceleration levels measured at three locations and the experiment is repeated for four driving point positions. The mass of each accelerometer is about 2 g and it is found that no correction for the mass of the accelerometers need be applied on the measured acceleration levels. The excitation force is measured using impedance head.

4.2. TOTAL LOSS FACTOR

Using equation (6) the loss factor of the panel is determined from the measured excitation force and the acceleration levels. Stationary broadband random excitation is used as the excitation force. To avoid frequency averaging, as suggested by Brown [15], a low value of resolution, 162·76 Hz, is adapted.

The parameter modal density, required while using equation (6) for determining the loss factor, is obtained theoretically. The modal density of the honeycomb sandwich panel with composite face sheet, incorporating the transverse shear deformation is given by [14]

$$n(f) = \frac{2ab\rho f}{N}\int_0^{\pi/2}\left\{\frac{f_2}{f_1} + \frac{1}{f_1}\left[\rho^2\omega^4 f_2^2 + \frac{4\rho\omega^2 N^2 f_1}{\sqrt{D_{11}D_{22}}}\right]^{-1/2}\left[\rho\omega^2 f_2^2 + \frac{2N^2 f_1}{\sqrt{D_{11}D_{22}}}\right]\right\}\mathrm{d}\theta, \quad (9)$$

where

$$f_1(\theta) = 1 - \gamma_1^2\sin^2(2\theta),\ f_2(\theta) = (D_{11}/D_{22})^{1/4}\cos^2\theta + (D_{22}/D_{11})^{1/4}\sin^2\theta \text{ and}$$

$$2\gamma_1^2 = 1 - (D_{12} + 2D_{66})/\sqrt{D_{11}D_{22}}. \quad (10)$$

The parameters D_{11}, D_{22}, D_{12} and D_{66} are the flexural rigidities of the panel and N is the shear rigidity. The pane is having dimensions a, b and ρ is its mass per unit area. The shear rigidity of a honeycomb sandwich panel is given by

$$N = G_c t_c\{1 + (t_f/t_c)\}^2, \quad (11)$$

where t_f is the thickness of the fact sheet, t_c is the thickness of the core and G_c is the shear modulus of the core. Since the modal density of a composite honeycomb sandwich panel estimated using equation (9) is in agreement with the experimental results [14, 16], use of theoretical results does not lead to any significant error in the derived loss factor values.

The loss factor thus obtained is shown in Figure 3. Since the experiment is conducted in air, the measured loss factor is the sum of the dissipation loss factor and the radiation loss factor [6], called total loss factor.

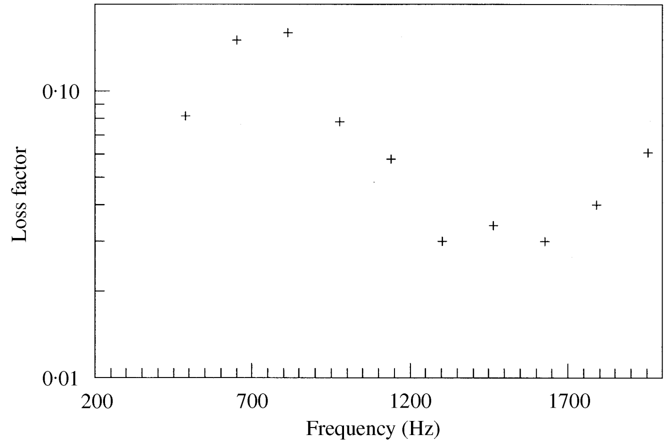

Figure 3. Total loss factor of the composite panel.

4.3. CRITICAL FREQUENCY

Critical frequency of a structure is the frequency at which the speed of the bending waves in the structure becomes equal to the speed of sound waves in air. For a thin plate, it is shown that

$$\omega_c^2 = c^4 \rho / D, \tag{12}$$

where ω_c is the critical frequency. Renji *et al.* [17] derived an expression for the critical frequency of a honeycomb sandwich panel with orthotropic face sheets as

$$\omega_c^2 = (c^4 \rho / D) / \{[(3 + \alpha)/4] - [c^2 \rho / N]\}, \tag{13}$$

where $D_{11} = D_{22} = D$ and $\alpha = (D_{12} + 2D_{66})/D$. The above expression considers transverse shear flexibility of the core and the orthotropic properties of the face sheets. Using equation (13) the critical frequency of the panel is estimated as 608 Hz. The speed of sound in air is assumed to be 346 m/s. The information on the critical frequency is necessary to determine the radiation loss factor.

4.4. RADIATION LOSS FACTOR

Since the experiment is conducted in air, one has to obtain the radiation loss factor of the structure to determine its dissipation loss factor. The radiation loss factor is theoretically determined using the following equations. The radiation loss factor denoted by η_{rad} is given by

$$\eta_{rad} = R_{rad} / (\omega \rho A), \tag{14}$$

where R_{rad} is the radiation resistance of the structure and A is the area of the panel. The radiation resistance of the panel is estimated using the following equations [18, 19].

For $f < f_c$ and ka, $kb > 2\pi$,

$$R_{rad} = A \rho_a c \{(\lambda_c \lambda_a / A) 2 (f/f_c) g_1 + (p \lambda_c / A) g_2\} / 2,$$

where

$$g_1 = (4/\pi^4)\{(1 - 2\psi^2) / [\psi (1 - \psi^2)^{1/2}]\} \quad \text{for } f/f_c < 0{\cdot}5,$$

$$g_1 = 0 \quad \text{for } f/f_c \geqslant 0{\cdot}5,$$

$$g_2 = (1/4\pi^2)\{(1 - \psi^2) ln[(1 + \psi)/(1 - \psi)] + 2\psi\} \{1/(1 - \psi^2)^{3/2}\},$$

$$\psi = (f/f_c)^{1/2}.$$

For $f < f_c$ and ka, $kb < 2\pi$,

$$R_{rad} = A \rho_a c (4/\pi^4)(p \lambda_c / A)(f/f_c)^{1/2} / 2.$$

For $f = f_c$,

$$R_{rad} = A \rho_a c \{(a/\lambda_c)^{1/2} + (b/\lambda_c)^{1/2}\} / 2.$$

For $f > f_c$,

$$R_{rad} = A \rho_a c \{1 - (f_c/f)\}^{-1/2}. \tag{15}$$

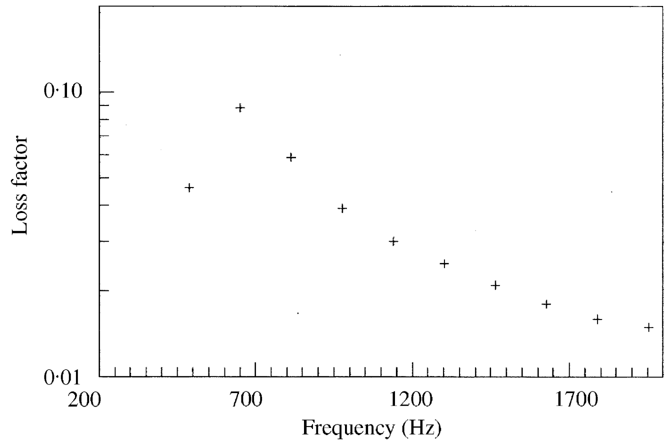

Figure 4. Estimated radiation loss factor of the composite panel.

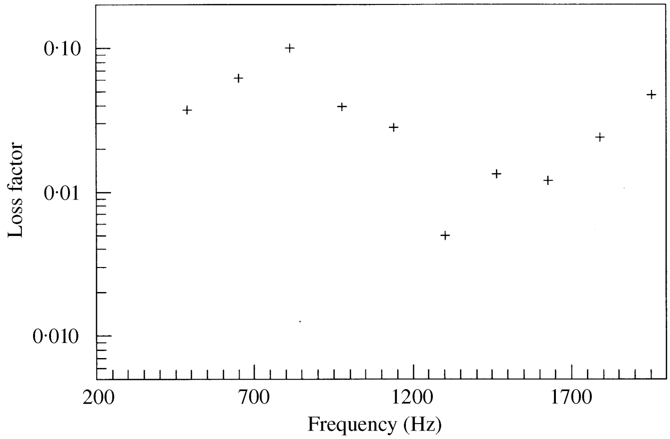

Figure 5. Dissipation loss factor of the composite panel.

In equation (15), p is the perimeter and f_c is the critical frequency of the panel. The wavelength of sound in air is denoted by λ_a and the wavelength at the critical frequency is λ_c. The density of air is denoted by ρ_a. The parameter k is the wavenumber in air.

The estimated radiation loss factor of the panel is shown in Figure 4. This is estimated using equation (15) for simply supported edge conditions. It is to be noted that the radiation loss factor of the panel is estimated assuming that the panel boundaries are having simple supports. However, in the present experiment the edges of the panel are free and at six points the panel is fixed. But the boundary conditions affect the radiation resistance only at low frequencies and at low frequencies the radiation resistance values are very small. Hence, use of the radiation resistance values estimated for simply supported boundaries does not cause any significant error in the dissipation loss factor values determined here.

4.5. DISSIPATION LOSS FACTOR

By subtracting the radiation loss factor from the total loss factor values, the dissipation loss factor of the panel is determined. The dissipation loss factor values are shown in Figure 5.

4.6. DISCUSSION OF RESULTS

It can be seen that the dissipation loss factor values are very small in the frequency range 1300–1600 Hz. It is to be noted that the measured driving forces are assumed to be the actual driving forces and no correction factors are applied. But the driving forces are measured using impedance head and due to the impedance of the impedance head and the attachment elements the measured force can be different from the actually applied force. This is investigated further.

5. EFFECT OF IMPEDANCE HEAD

5.1. THEORY

The excitation force is measured using impedance head. The impedance of the impedance head and the attachment elements influence the measured force. This means that the measured force will be different from the actually applied force.

Following the analysis by Brown and Norton [12], the actual force, denoted by f_a, is given by

$$f_a = f_m/\{1 + (Y/Y_M)\}, \tag{16}$$

where f_m is the measured force, Y is the driving point admittance and Y_M is the admittance due to the impedance head the attachment elements. The parameter Y_M could be determined by exciting the impedance head and the attaching stud. If M is the mass of the impedance head and the attachment elements, its admittance is given by

$$Y_M = 1/(j\omega M). \tag{17}$$

The above equation is valid for a wide frequency range upto the frequency of resonance of the impedance head and the attachment elements.

The driving point admittance, in general, can have both real and imaginary parts and hence the expression for the actual force becomes

$$f_a = f_m/\{1 + [\mathrm{Re}(Y)_{+}\mathrm{jIm}(Y)]/Y_M)\}, \tag{18}$$

where $\mathrm{Re}(Y)$ is the real part of the admittance and $\mathrm{Im}(Y)$ is the imaginary part of the admittance. Substituting equation (17) in equation (18) we get

$$f_a = f_m/\{1 - \omega M \,\mathrm{Im}(Y) + \mathrm{j}\omega M \mathrm{Re}(Y)\}. \tag{19}$$

The above equation can be rewritten as

$$f_a = f_m\{1 - \omega M \mathrm{Im}(Y) - \mathrm{j}\omega M \mathrm{Re}(Y)\}/\{[1 - \omega M \,\mathrm{Im}(Y)]^2 + [\omega M \mathrm{Re}(Y)]^2\}. \tag{20}$$

The magnitude of the actual force can then be obtained as

$$|f_a| = |f_m|\{[1 - \omega M \,\mathrm{Im}(Y)]^2 + [\omega M \,\mathrm{Re}(Y)]^2\}^{1/2}/\{[1 - \omega M \,\mathrm{Im}(Y)]^2 + [\omega M \,\mathrm{Re}(Y)]^2\}. \tag{21}$$

The mean square value of the actual force is then given by

$$f_a^2 = f_m^2/\{[1 - \omega M \,\mathrm{Im}(Y)]^2 + [\omega M \,\mathrm{Re}(Y)]^2\}. \tag{22}$$

This means that to determine the actual force from the measured force, it is necessary to measure the driving point admittance, both the real and the imaginary parts.

Driving point admittance is the ratio of the Fourier transform of the velocity of the driving point to the Fourier transform of the driving force. The admittance can be determined using the relation

$$Y = \phi_{fv}/\phi_{ff}, \tag{23}$$

where ϕ_{ff} is the auto-spectral density of the force and ϕ_{fv} is the cross-spectral density between the force and the velocity. Clarkson and Pope [9] had reported that the measured driving point admittance values were influenced by the admittance of the impedance head and the attachment elements. To take into account this effect, Brown and Norton [12] suggested the use of a correction factor as given below:

$$Y_a = Y_m/\{1 - (Y_m/Y_M)\}, \tag{24}$$

where Y_a is the actual admittance and Y_m is the measured admittance. Hence, the equation for the actual force becomes

$$f_a^2 = f_m^2/\{[1 - \omega M \operatorname{Im}(Y_a)]^2 + [\omega M \operatorname{Re}(Y_a)]^2\}. \tag{25}$$

It remains now to find out the imaginary and real parts of the actual driving point admittance. Using equation (17) for the admittance of the impedance head and the attachment elements, the actual admittance can be determined from the measured admittance using equation (24) as

$$Y_a = Y_m/\{1 - \mathrm{j}\omega M Y_m\}. \tag{26}$$

The measured admittance can have real and imaginary parts, that is $Y_m = \operatorname{Re}(Y_m) + \mathrm{j}\operatorname{Im}(Y_m)$, and hence expression for the actual admittance in terms of the measured admittance becomes

$$Y_a = \{\operatorname{Re}(Y_m) + \mathrm{j}\operatorname{Im}(Y_m)\}\{1 + \omega M \operatorname{Im}(Y_m) + \mathrm{j}\omega M \operatorname{Re}(Y_m)\}/\{[1 + \omega M \operatorname{Im}(Y_m)]^2 + [\omega M \operatorname{Re}(Y_m)]^2\}. \tag{27}$$

Hence, the real and the imaginary parts of the actual admittance are given by

$$\operatorname{Re}(Y_a) = \operatorname{Re}(Y_m)/\{[1 + \omega M \operatorname{Im}(Y_m)]^2 + [\omega M \operatorname{Re}(Y_m)]^2\}. \tag{28}$$

$$\operatorname{Im}(Y_a) = [\omega M\{\operatorname{Re}^2(Y_m) + \operatorname{Im}^2(Y_m)\} + \operatorname{Im}(Y_m)][\operatorname{Re}(Y_a)/\operatorname{Re}(Y_m)]. \tag{29}$$

The actual force can be determined from the measured force using equations (28) and (29) in equation (25).

5.2. TEST RESULTS

Using equation (6), the loss factor of the panel is determined from the measured driving force and the acceleration levels. The tests conducted are the same as those discussed previously, but the driving point admittance values are also obtained.

The driving point admittance is obtained by measuring the force and acceleration at the driving point. From the above signals the cross-spectral densities of velocity and force are calculated. The driving point admittance is then obtained using equation (23). It was discussed earlier that the measured admittance could be in error due to the admittance of

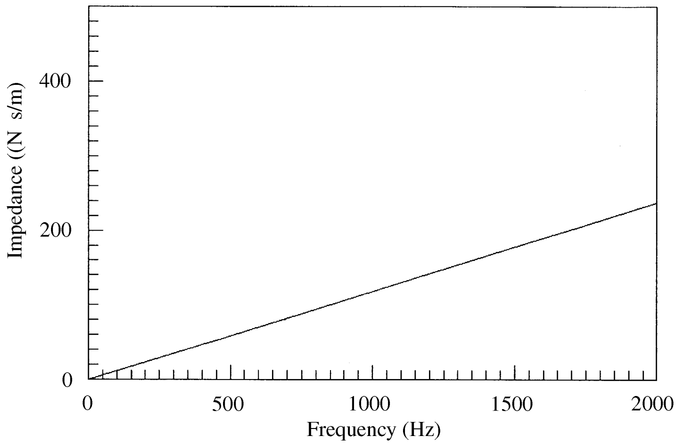

Figure 6. Impedance of the impedance head and the attachment elements.

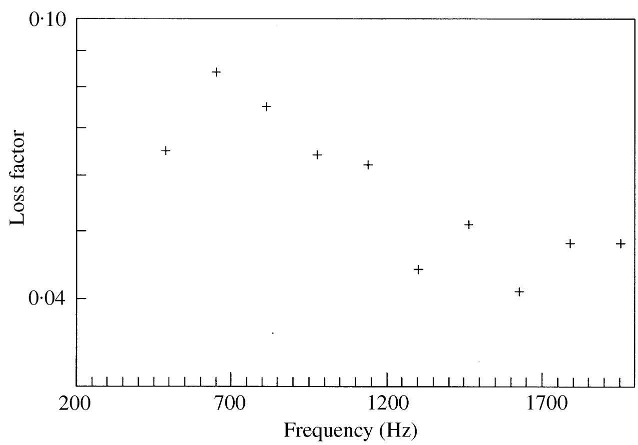

Figure 7. Total loss factor of the composite panel with force corrections.

the impedance head and the attachment elements and the actual admittance is given by equations (28) and (29). To apply the corrections, the impedance of the impedance head and the attachment elements should be evaluated. The measured impedance of the impedance head and the attachment elements used in the present experiment is shown in Figure 6. At 2000 Hz, the impedance is about 237 N s/m and it can be seen from the results that the admittance follow the relation given by equation (17). For calculating the actual admittance using equations (28) and (29), the value of Y_M averaged over 162·76 Hz bandwidth is used. Thus, from the measured values of driving force, driving point acceleration and the impedance of the impedance head, the real and the imaginary parts of the actual driving point admittance values are obtained by using equations (23), (28) and (29).

From the measured values of the driving forces and known values of the real and imaginary parts of the actual driving point admittance, the actually applied forces are calculated using equation (25). The total loss factor is then determined using equation (6) and the results are shown in Figure 7. The radiation loss factor of the panel is as shown in Figure 4. By subtracting the radiation loss factor from the total loss factor, the dissipation loss factor of the panel is determined and the results are shown in Figure 8.

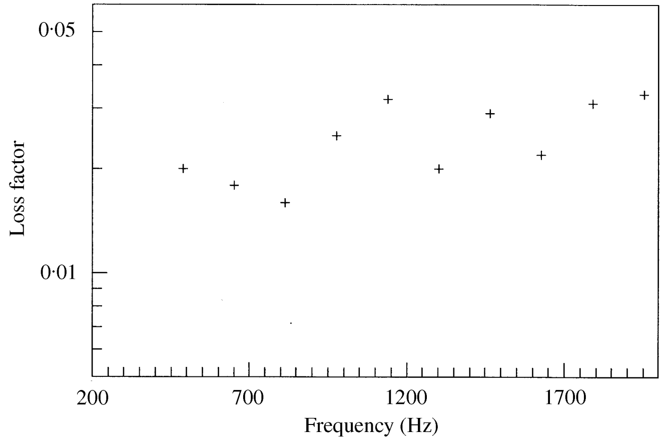

Figure 8. Dissipation loss factor of the panel with force corrections.

It can be observed from Figures 7 and 4 that the measured dissipation loss factor near the critical frequency is very low. This is because the radiation loss factor is very large near the critical frequency and the dissipation loss factor is relatively low. Hence the total loss factor is approximately same as the radiation loss factor and the difference between them is not expected to be accurate. Hence, at this frequency the average of the dissipation loss factors of the nearby frequency bands is used.

5.3. DISCUSSION OF RESULTS

It can be seen from the results given in Figure 8 that the dissipation loss factor is almost constant in the entire frequency band. The energy average of the dissipation loss factors in the entire frequency band is equal to 0·027. These values are approximately same as those for the panels with aluminium face sheets. If an accurate estimate of the dissipation loss factor is required one can use different values in the lower and higher frequencies. In such a case following values can be used as dissipation loss factors of honeycomb sandwich panels with composite face sheets:

up to 1414 Hz 0·022,
(upper limit of 1000 Hz octave band)

above 1414 Hz 0·034.

As discussed earlier, the actual forces are different from the measured forces. The effect is more significant at high frequencies than at low frequencies. To have a feel of the difference between the actual force and the measured force, the results at driving point 5 are given in Figure 9. One can observe the differences in the measured and the actual forces and their significance.

It is interesting to see the results of the dissipation loss factors if the corrections are not applied on the measured forces, that is Figure 5. The dissipation loss factor is very low for a small frequency range near 1300 Hz, if the correction factors are not applied. The results show that to determine accurate values of input force and hence the dissipation loss factor, correction on the measured force is necessary. To arrive at the correction, both the real and

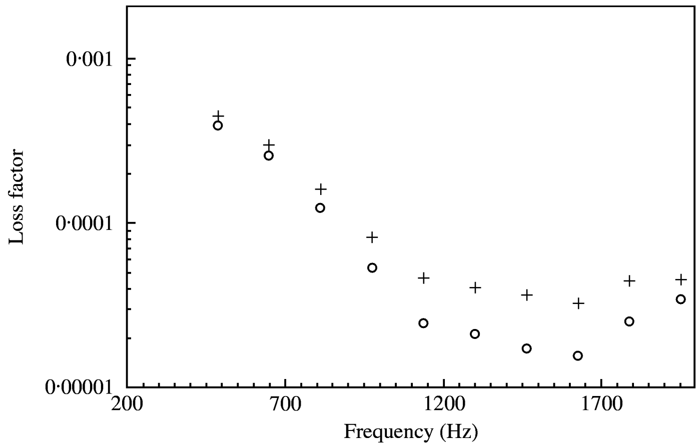

Figure 9. Actual and measured forces at location 2: +, actual force; ○, measured force.

the imaginary parts of the driving point admittance have to be measured and equation (25) to be used.

A detailed investigation reveals that the above behaviour occurs at frequencies near the frequency of the fundamental mode of the vibration of the core cell. The fundamental mode of core cell vibration is estimated to be 1520 Hz. This is the frequency of the first mode of bending vibration of the cell wall for simply supported boundaries.

The radiation loss factor is very large at frequencies near the critical frequency. Near the critical frequency of a panel the total loss factor increases to a large value. Based on the above characteristics the critical frequency of a panel can be found out experimentally from the measured total loss factor. The critical frequency of the panel used in the present experiment is found to be 651 Hz. The experimental results validate the expression for the critical frequency given by equation (13) derived earlier [17]. Although the experimental results were provided in reference [17], the loss factor was determined from one driving point position. The present experiment is conducted with four driving point positions. Hence, the present results are expected to be more reliable. The results also show that the critical frequency can be determined even with one driving point without loss of accuracy. However, the single driving point used in the experiment is not at the boundary or a symmetric point. Also, there are a large number of modes in the frequency band near the critical frequency [14]. If the driving point is at the boundary, the results will not be reliable. The total loss factor determined by exciting at corner of the panel is shown in Figure 10. It can be seen that the critical frequency cannot be determined from that data.

6. CONCLUSIONS

Dissipation loss factor of a typical honeycomb sandwich panel with composite sheets is obtained experimentally using the energy method. The dissipation loss factors of the composite panel are approximately the same as those of the panels with aluminium face sheets. The measured driving force is influenced by the impedance of the impedance head and the attachment elements. In order to determine the actual driving force, a correction factor has to be applied on the measured driving force to take into account the impedance of the impedance head and the attachment elements. An expression for this correction factor is

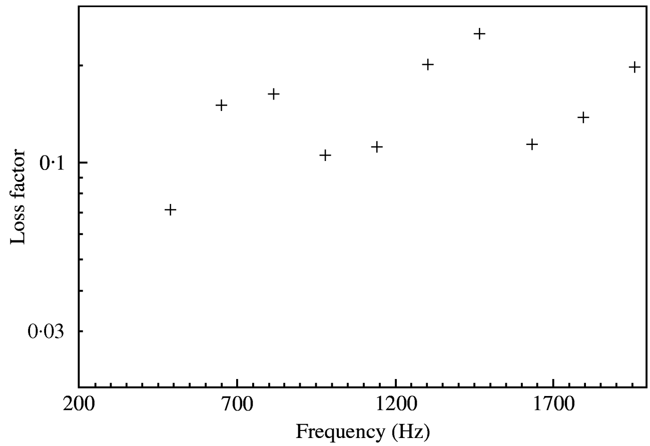

Figure 10. Total loss factor of the panel with driving point at the corner.

developed. It is seen that failure to incorporate the above-mentioned corrections can give largely different dissipation loss factor values compared to the actual values. The experimental results validate the expression derived earlier for the critical frequency of honeycomb sandwich panels considering the transverse shear deformation effects and the orthotropic properties of the face sheets.

ACKNOWLEDGMENT

The authors wish to thank Dr P. S. Nair, Group Director, Structures, ISRO Satellite Centre for his valuable suggestions.

REFERENCES

1. R. H. LYON 1975 *Statistical Energy Analysis of Dynamical Systems: Theory and Applications*. Cambridge, MA: MIT Press.
2. J. G. VAN BAKEL and D. DE VRIES 1983 *Journal of Sound and Vibration* **90**, 373–380. Parameter sensitivity of a T-junction SEA model: the importance of the internal damping loss factors.
3. R. J. CUMMINS and I. R. FARROW 1981 ESA CR(P)-1609, Vol. 2. Study of the evolution of the structural acoustic design guides.
4. D. C. G. EATON 1987 ESA PSS-03-1201 Issue 1. Structural acoustic design manual.
5. M. F. RANKY and B. L. CLARKSON 1983 *Journal of Sound and Vibration* **89**, 309–323. Frequency average loss factors of plates and shells.
6. B. L. CLARKSON and K. T. BROWN 1985 *Transactions of the American Society of Mechanical Engineers Journal of Vibration, Acoustics, Stress and Reliability in Design* **107**, 357–360. Acoustic radiation damping.
7. T. D. SCHARTON and R. H. LYON 1968 *Journal of Acoustical Society of America* **43**, 1332–1343. Power flow and energy sharing in random vibration.
8. B. L. CLARKSON 1981 *Journal of Sound and Vibration* **77**, 583–584. The derivation of modal densities from point impedances.
9. B. L. CLARKSON and R. J. POPE 1981 *Journal of Sound and Vibration* **77**, 535–549. Experimental determination of modal densities and loss factors of flat plates and cylinders.
10. M. P. NORTON and R. GREENHALGH 1986 *Journal of Sound and Vibration* **105**, 397–423. On the estimation of loss factors in lightly damped pipeline systems: some measurement techniques and their limitations.

11. D. A. BIES and S. HAMID 1980 *Journal of Sound and Vibration* **70**, 187–204. In situ determination of loss and coupling loss factors by the power injection method.
12. K. T. BROWN and M. P. NORTON 1985 *Journal of Sound and Vibration* **102**, 588–594. Some comments on the experimental determination of modal densities and loss factors for statistical energy analysis applications.
13. B. L. CLARKSON and M. F. RANKY 1983 *Journal of Sound and Vibration* **91**, 103–118. Modal density of honeycomb plates.
14. K. RENJI, P. S. NAIR and S. NARAYANAN 1996 *Journal of Sound and Vibration* **195**, 687–699. Modal density of composite honeycomb sandwich panels.
15. K. T. BROWN 1984 *Journal of Sound and Vibration* **96**, 127–132. Measurement of modal density: an improved technique for use on lightly damped structures.
16. K. RENJI 2000 *Journal of Sound and Vibration* **237**, 67–79. Experimental modal densities of honeycomb sandwich panels at high frequencies.
17. K. RENJI, P. S. NAIR and S. NARAYANAN 1997 *Journal of Sound and Vibration* **205**, 19–32. Critical and coincidence frequencies of flat panels.
18. G. MAIDANIK 1962 *Journal of the Acoustical Society of America* **34**, 809–826. Response of ribbed panels to reverberant acoustic fields.
19. K. RENJI, P. S. NAIR and S. NARAYANAN 1998 *Journal of Sound and Vibration* **212**, 583–598. On acoustic radiation resistance of plates.

APPENDIX A: NOMENCLATURE

Symbols not listed here are used only at specific places and are explained wherever they occur.

a, b	dimensions of a panel
A	area of the plate
c	speed of sound in air
$D_{11}, D_{22}, D_{12}, D_{66}, D$	flexural rigidity values of a laminate
DR	decay rate
E	twice the mean kinetic energy
f	frequency, in Hz
f_a	actual force
f_c	critical frequency, in Hz
f_m	measured force
f_n	natural frequency, in Hz
f_p	applied force
G_c	shear modulus of the core
$\mathrm{Im}(x)$	imaginary part of the variable x
j	complex operator
k	wavenumber in air
M	mass of impedance head and the attachment elements
m	mass of a panel
N	shear rigidity of a panel
$n(f)$	number of modes per Hz
p	perimeter of a plate
R_{rad}	radiation resistance
$\mathrm{Re}(x)$	real part of x
t_c	thickness of the core
t_f	thickness of the face sheet
T_{60}	reverberation time
v	velocity of the structure
v^2	mean square value of the velocity
Y	driving point admittance
Y_a	actual driving point admittance
Y_M	admittance of the impedance head and attachment elements
Y_m	measured driving point admittance
Δ	half-power bandwidth

η_d	dissipation loss factor
η_{rad}	radiation loss factor
λ_a	wavelength in air
λ_c	wavelength at critical frequency
ϕ_{xy}	cross-spectral density between the random processes x and y
π_d	dissipated power
π_{in}	input power
ω	circular frequency, in rad/s
ω_c	critical frequency, in rad/s
ρ	mass per unit area
ρ_a	density of air
$\langle\rangle_x$	average over the domain x